# Peatlands Versus Permafrost: Landscape Features as Drivers of Dissolved Organic Matter Composition in West Siberian Rivers

**Sommer F. Starr[1]** [ID], **Karen E. Frey[2]** [ID], **Laurence C. Smith[3]** [ID], **Anne M. Kellerman[1]** [ID], **Amy M. McKenna[4,5]** [ID], **and Robert G. M. Spencer[1]** [ID]

[1]National High Magnetic Field Laboratory Geochemistry Group and Department of Earth, Ocean, and Atmospheric Science, Florida State University, Tallahassee, FL, USA, [2]Graduate School of Geography, Clark University, Worcester, MA, USA, [3]Department of Earth, Environmental, and Planetary Sciences, Brown University, Institute at Brown for Environment and Society, Providence, RI, USA, [4]National High Magnetic Field Laboratory FT-ICR MS Group, National High Magnetic Field Laboratory, Tallahassee, FL, USA, [5]Department of Soil and Crop Sciences, Colorado State University, Fort Collins, CO, USA

**Abstract** West Siberia contains some of the largest soil carbon stores on Earth owing to vast areas of peatlands and permafrost, with the region warming far faster than the global average. Organic matter transported in fluvial systems is likely to undergo distinct compositional changes as peatlands and permafrost warm. However, the influence of peatlands and permafrost on future dissolved organic matter (DOM) composition is not well characterized. To better understand how these environmental drivers may impact DOM composition in warming Arctic rivers, we used ultrahigh resolution Fourier-transform ion cyclotron resonance mass spectrometry to analyze riverine DOM composition across a latitudinal gradient of West Siberia spanning both permafrost-influenced and permafrost-free watersheds and varying proportions of peatland cover. We find that peatland cover explains much of the variance in DOM composition in permafrost-free watersheds in West Siberia, but this effect is suppressed in permafrost-influenced watersheds. DOM from warm permafrost-free watersheds was more heterogenous, higher molecular weight, and relatively nitrogen enriched in comparison to DOM from cold permafrost-influenced watersheds, which were relatively enriched in energy-rich peptide-like and aliphatic compounds. Therefore, we predict that as these watersheds warm, West Siberian rivers will export more heterogeneous DOM with higher average molecular weight than at present. Such compositional shifts have been linked to different fates of DOM in downstream ecosystems. For example, a shift toward higher molecular weight, less energy-rich DOM may lead to a change in the fate of this material, making it more susceptible to photochemical degradation processes, particularly in the receiving Arctic Ocean.

**Plain Language Summary** West Siberia is warming faster than other regions and contains vast areas of peatlands and permafrost, which contain vast stores of carbon. This carbon is transported off the landscape by rivers and the composition of this exported carbon is likely to change with continued warming, but there is no consensus on exactly what changes will occur. To study these potential changes, we used ultrahigh resolution mass spectrometry to analyze molecular-level organic matter composition across a gradient of permafrost influence and peatland cover in West Siberian watersheds. Warm permafrost-free watersheds had organic matter that was more diverse, of higher molecular weight, and had unique molecular composition compared to cold permafrost-influenced watersheds. We also found that while peatland cover explained much of the compositional diversity between rivers, permafrost ultimately controlled the influence of peatland cover on dissolved organic matter composition, effectively acting as a switch on the compositional signal from peatlands. We predict that as West Siberia warms, the fate of organic matter transported by rivers in the region will thus change and the role of photochemical degradation processes may become more important.

## 1. Introduction

Northern peatland and permafrost soils are two of the Earth's most significant reservoirs of organic carbon (OC), storing approximately 415 and 1,500 Pg C, respectively (Hugelius et al., 2020; Schuur et al., 2015). These stores are facing rapid warming, with a projected release of up to hundreds of Pg C over the coming century (Natali et al., 2021; Schuur et al., 2013, 2022). Rivers receiving OC from these landscapes carry geochemical signatures that can provide insights into how these ecosystems are changing (Behnke et al., 2021; Frey, McClelland

et al., 2007, Frey, Siegel, et al., 2007; Spencer et al., 2015; Wild et al., 2019). The majority of OC transported by Arctic streams and rivers is in the dissolved phase, and the concentration and characteristics of dissolved organic matter (DOM) exported to the Arctic Ocean has implications for food webs, biogeochemical processes, and climate change feedbacks (Fabre et al., 2019; Kaiser et al., 2017; Terhaar et al., 2021). Specifically, changes in riverine DOM composition and thus biolability have the potential to alter both primary production and respiration in marine ecosystems (Behnke et al., 2021; Clark et al., 2022). Rapid warming is changing both the amount and composition of exported DOM, but the exact nature of these changes is still not fully characterized (Behnke et al., 2021; Frey & McClelland, 2009). While many studies have examined the impact of either permafrost influence or peatland cover (i.e., the percentage of the watershed covered by peatland) on exported DOM (e.g., Sepp et al., 2019; Spencer et al., 2007, 2015; Stubbins et al., 2017; Xenopoulos et al., 2003), relatively few have sought to consider the influence and interaction of both factors (e.g., Frey & Smith, 2005; Gandois et al., 2019; Walker et al., 2013), despite the fact that nearly half of stored peatland OC is influenced by permafrost (Hugelius et al., 2020; Schuur et al., 2015). Understanding the impact and interplay of permafrost influence and peatland cover on riverine DOM export is thus necessary for understanding how warming landscapes may alter the Arctic carbon cycle.

DOM represents a compositionally complex and polyfunctional mixture of organic compounds that spans a range of molecular weights. The composition of DOM in surface waters reflects the terrestrial attributes that rivers traverse, including wetland area, soil type, and land cover (Mann et al., 2014). Many of the molecular formulae that comprise DOM contain bioavailable components that can be used for microbial metabolism and support coupled biogeochemical processes like denitrification (Barnes et al., 2012). The degradation of DOM is affected by abiotic environmental factors (i.e., temperature, nutrient availability, redox conditions) and by the chemical composition of the DOM itself. For example, highly aromatic, high molecular weight compounds have been suggested to be less available for biodegradation and are more likely to be stored on longer time scales once exported to marine environments (Behnke et al., 2021; Benner et al., 2005; Jiao et al., 2010). However, these aromatic components may be more susceptible to photochemical degradation, especially once exported into the coastal ocean (Bowen et al., 2020; Grunert et al., 2021; Ward & Cory, 2016). Conversely, energy-rich aliphatic compounds and low molecular weight components of the DOM pool have been often observed to be highly susceptible to biodegradation and subject to rapid degradation in oxygenated waters (D'Andrilli et al., 2015; Drake et al., 2015; Jiao et al., 2010; Spencer et al., 2015). Therefore, understanding the composition and thus reactivity of the source material is important for understanding the fate of DOM exported from the landscape.

Permafrost exerts strong controls on hydrology, affecting both surface and groundwater flow, and on dissolved OC (DOC) concentration and DOM composition (Juhls et al., 2020; Lin et al., 2021; O'Donnell et al., 2016). Permafrost thaw releases stored OC and impacts the mobilization and processing of DOM from terrestrial systems into, and through, aquatic systems (Schuur et al., 2008; Striegl et al., 2005). It has been suggested that in West Siberia specifically, permafrost exerts influence over DOC transport by regulating the impact of groundwater flow and the leaching of organic material from the active soil layer (Frey & Smith, 2005; Frey, McClelland et al., 2007; McClelland, et al., 2007; Pokrovsky et al., 2015). Permafrost-derived DOM typically has a molecular-level composition characterized by a high relative abundance (RA) of energy-rich aliphatic compounds and past research has attributed the rapid biodegradation of permafrost-derived DOM to its distinct aliphatic signature (Drake et al., 2018; Spencer et al., 2015; Textor et al., 2019). As permafrost thaw continues, it is important to understand how other landscape variables that affect biogeochemical cycling (e.g., peat cover) may impact DOM generation, composition, and export in changing permafrost environments.

Peatland cover is one of the best indicators of DOC concentrations in surface waters globally (Aitkenhead & McDowell, 2000; Xenopoulos et al., 2003) and in Arctic and boreal systems, specifically (Frey & Smith, 2005; Hall et al., 2021; Kortelainen et al., 2006). DOC concentration increases with peatland area in watersheds, with peatland influence explaining as much as 75% of OC export in some catchments (Kortelainen et al., 2006). Peatland DOM is typically characterized by high molecular weight and aromatic compounds, and is typically of relatively recent age (Chanton et al., 2008; Tfaily et al., 2013). Peatlands currently act as net carbon sinks (Loisel et al., 2020; Smith et al., 2004), but some projections estimate that peatlands will become either net carbon sources and/or net sources of radiative forcing under continued warming through the release of greenhouse gases (Friborg et al., 2003; Frolking et al., 2011; Hugelius et al., 2020). Some predictions assert that as a whole, Arctic peatlands will continue to act as net carbon sinks under future warming (Chaudhary et al., 2020; Gallego-Sala et al., 2018), or under certain warming scenarios (Qiu et al., 2022). However, predicting whether overall peatland area may

shrink or expand with future human impacts is difficult both because of the high variability in hydrology and terrain across the Arctic as well as a dearth of available data (Chaudhary et al., 2020; Fewster et al., 2022; Morris et al., 2018). Furthermore, previous research suggests that interactions between permafrost and peatland may create unique impacts on DOC export, but further research is necessary to understand the impacts of these interactions on DOM composition (Frey & Smith, 2005). Because of this uncertainty in the role of Arctic peatlands in OC processing under continued global change, it is important to examine their impacts on DOM composition and export and potential interactions between permafrost and peatlands where they occur concurrently to better understand how the role of northern high-latitude peatlands in the global carbon cycle may shift in the future.

The West Siberian Lowland contains the largest expanse of frozen peatlands in the world (Pokrovsky et al., 2015, 2020) with an estimated carbon storage of $\sim 47 \pm 23$ kg C m$^{-2}$ (Lim et al., 2022), but this carbon-rich region is warming faster than the rest of the Arctic (Frey & Smith, 2005). The Intergovernmental Panel on Climate Change predicts both a warmer and wetter shift for Siberian climate (IPCC, 2023), suggesting an increase in annual runoff from Siberian rivers and streams. Long-term increases in DOC concentration in boreal regions have been attributed to greater primary production because of warming and elevated atmospheric $CO_2$ and increased rates of permafrost thaw (Fenner et al., 2009; Moore, 2009). Increases in both runoff and DOM production suggest that warming may enhance the amount of DOM exported from the landscape via Siberian rivers. This increase in DOM export can be expected to occur concurrently with shifts in DOM composition and thus reactivity, but the exact nature of these changes is not well constrained. Therefore, the uncertainty with respect to the fate of Siberian riverine DOM calls for increased research efforts into DOM composition and its controls in the region.

Here, we examine riverine DOM along gradients of permafrost and peatland cover in West Siberia to explore the likely impacts of climate warming on DOM composition. We examine permafrost-influenced and permafrost-free watersheds with similar distributions of peatland cover, allowing for the analysis of concurrent peatland cover and permafrost influence effects on DOM. This "substitute-space-for-time" approach has previously been used in West Siberia (Frey & Smith, 2005; Frey, McClelland, et al., 2007, Frey, Siegel, et al., 2007; Smith et al., 2005) and allows projection of potential changes in DOM composition under future warming scenarios. Previous studies focused on West Siberia have examined DOC concentration and optical parameters to assess bulk DOM composition (Frey & Smith, 2005; Lim et al., 2022; Raudina et al., 2017). Here, we utilize ultrahigh resolution DOM compositional data to expand on these previous observations by examining how shifts driven by permafrost cover and peatland inputs in West Siberian watersheds impact DOM at the molecular level and subsequently infer how these compositional shifts may impact the fate of exported riverine DOM. The sub-parts per million mass measurement accuracy, precision, and mass resolving power (m/$\Delta$m$_{50\%}$ > 2,000,000 at $m/z$ 400) of Fourier-transform ion cyclotron resonance mass spectrometry (FT-ICR MS) at 21 T coupled with negative-ion electrospray ionization enables assignment of tens of thousands of molecular formulae providing insight into West Siberian DOM composition and cycling (Behnke et al., 2021; Kellerman et al., 2015; Roth et al., 2022), enabling a comprehensive assessment of how permafrost and peatlands may impact riverine DOM composition in West Siberia. We hypothesize that in permafrost-free watersheds, peatland cover will lead to greater variability in DOM composition as previously noted for DOC concentration (Frey & Smith, 2005). Furthermore, as permafrost has been shown to have a distinct molecular-level DOM composition, we hypothesize that permafrost-influenced watersheds will exhibit unique compositional signatures, for example, enrichment in aliphatic moieties.

## 2. Methods

### 2.1. Study Site and Sample Collection

Water samples were collected from streams and rivers across West Siberia during the late-summer periods of 2000 and 2001 as described in Frey and Smith (2005). This sampling effort covered catchments ranging from 38 km$^2$ to $\sim$2,700,000 km$^2$. Collected water samples were filtered in the field through Osmonics 0.22 micron mixed ester membranes and stored in acid-washed high density polyethylene bottles at $-20°C$ until analysis. A total of 73 samples collected across a latitudinal gradient from $\sim$55 to 68° N were used in this study, sampling 20 cold permafrost-influenced (CPI) and 53 warm permafrost-free (WPF) watersheds (Figure 1). Delineations of these watershed types were established using the southern limit of permafrost as mapped by Brown (1998). DOC concentrations from these samples were previously reported in Frey and Smith (2005) but duplicate samples were frozen and maintained at the University of California, Los Angeles. In 2022 the stored samples were transferred to Florida State University for DOM compositional analysis.
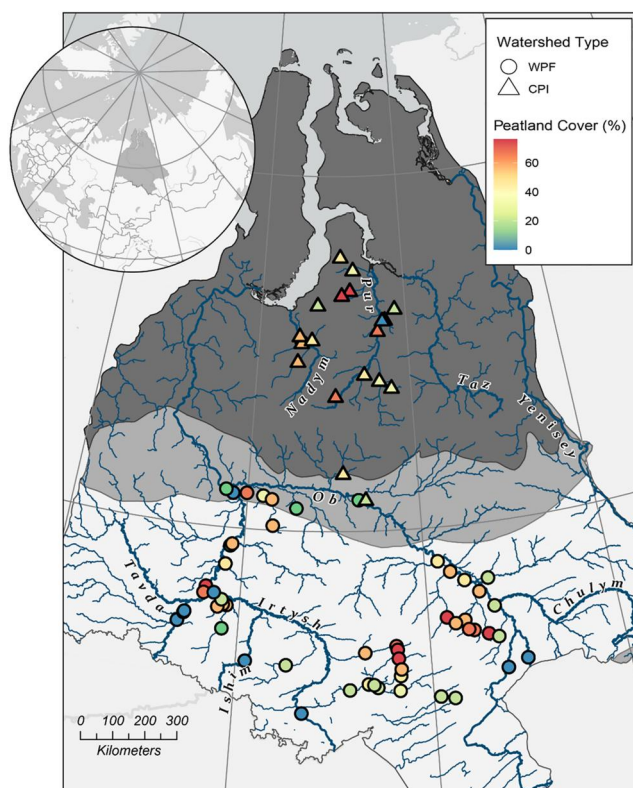
**Figure 1.** Map showing the sampling sites in West Siberia. Warm permafrost-free watersheds are depicted as circles and cold permafrost-influenced watersheds are depicted as triangles. The color of the points represents peatland cover (%), where cooler colors (blue) indicate less peatland cover and warmer colors (red) indicate greater peatland cover. Regions without permafrost, with isolated permafrost, and with continuous and discontinuous permafrost are displayed from bottom to top respectively in light, medium, and dark gray. River networks are symbolized with blue lines.

## 2.2. GIS Landcover Delineation

As previously outlined in Frey and Smith (2005), watershed boundaries were delineated using the Digital Chart of the World drainage network data, the GTOPO30 digital elevation model, U.S. Tactical Pilotage Charts, U.S. Operational Navigation Charts, and Russian Oblast maps in ESRI ArcGIS v. 8.0. The percentage of peatland cover for each watershed was calculated using a geographic information system-based inventory of peatlands in the region (Sheng et al., 2004; Smith et al., 2004) and mean annual air temperature (MAAT) was calculated for each watershed using gridded climate normal for 1961–1990 (New et al., 1999).

## 2.3. Solid Phase Extractions

DOM from filtered water samples was isolated using solid phase extraction onto individual PPL cartridges (Agilent Technologies) in preparation for negative-ion electrospray ionization FT-ICR MS analysis. PPL cartridges were prepared for extractions using established protocols (Johnston et al., 2018); specifically, the polymer was first soaked in methanol (high-performance liquid chromatography grade) for at least 4 hr, followed by two rinses with ultrapure water, one rinse with methanol, and two more rinses with acidified ultrapure water (to pH 2). Filtered samples were acidified to pH 2 with 12 M HCl before 50 μg C equivalent aliquots were extracted onto 100 mg PPL cartridges and eluted with methanol into precombusted (550°C, > 5h) vials to a final concentration of 50 μg OC mL$^{-1}$ following established methods (Dittmar et al., 2008). Eluted samples were kept cold (−20°C) at Florida State University prior to 21 T FT-ICR MS analysis.

## 2.4. Negative-Ion Electrospray Ionization 21 T FT-ICR MS

Solid-phase extracted DOM eluents were analyzed at the National High Magnetic Field Laboratory in Tallahassee, Florida on a custom-built hybrid/linear ion trap FT-ICR MS equipped with a 21 T superconducting solenoid magnet (Hendrickson et al., 2015; Smith et al., 2018) with negative electrospray ionization (ESI; 50 μm i.d. fused silica emitter at 500 nL/min). Typical conditions for negative ion formation: emitter voltage: −2.0–2.8 kV; S-lens RF level: 40%; heated metal capillary temperature: 350°C; at a flow rate of 500 nL min$^{-1}$. Acquired mass spectra were obtained by coadding 100 individual 3.1 s transients for each mass spectrum and phase-corrected (Xian et al., 2010). Mass spectral peaks with a signal magnitude greater than six-times the baseline noise level (6σ) were converted to Kendrick mass scale and internally calibrated with 10–15 highly abundant homologous series spanning the entire molecular weight distribution based on the "walking" calibration method (Savory et al., 2011). Elemental composition assignment was performed with PetroOrg©,™ (Corilo, 2015) with heteroatom constraints: $C_{1-100}H_{4-200}O_{1-25}N_{0-2}S_{0-1}$ and <200 ppb mass error Blakney et al., 2011. There were a total of 30,812 molecular formulae assigned across the entire sample set, with a molecular formulae assignment of >90% across all samples. All 21 T FT-ICR MS raw files, calibrated peak lists, and elemental compositions are publicly available via the Open Science Framework at https://osf.io/ via DOI 10.17605/OSF.IO/Q46TS.

Compound classes were defined based on elemental ratios and modified aromaticity indices (AI$_{mod}$) calculated from the neutral elemental composition (Koch & Dittmar, 2006, 2015). These classes were defined as: (a) highly unsaturated and phenolic (HUP), low O/C ratio (AI$_{mod}$ < 0.5, H/C < 1.5, O/C < 0.5), (b) HUP, high O/C ratio (AI$_{mod}$ < 0.5, H/C < 1.5, O/C ≥ 0.5), (c) aliphatic (H/C ≥ 1.5, $N = 0$), (d) condensed aromatic (AI$_{mod}$ ≥ 0.67), (e) polyphenolic (0.67 > AI$_{mod}$ > 0.5), and (f) peptide-like (H/C ≥ 1.5, $N > 0$) (Kellerman et al., 2015). Relative abundances of each formula were determined by normalizing the magnitude of each peak relative to the sum of all assigned peaks in each sample. The nominal oxidation state of carbon (NOSC) was determined using the equation presented in Riedel et al. (2012):

$$NOSC = 4 - \left[\frac{4c + h - 3n - 2o - 2s}{c}\right]$$

where $c$, $h$, $n$, $o$, and $s$ refer to the number of atoms of carbon, hydrogen, nitrogen, oxygen, and sulfur, respectively per molecular formula, assuming that all elements other than carbon are in their initial oxidation states. Contributions of both elemental composition (e.g., CHO, CHON, CHOS, CHONS) and compound class to detected composition (as % RA or %RA) were then calculated as the sum of all the relative abundances of each peak defined as a given elemental composition or compound class divided by the summed abundances of all assigned formulae.

### 2.5. Statistical Analysis

Principal component analysis (PCA) was conducted using the "vegan" package in R (Oksanen et al., 2020). Sample variances ($s^2$) were calculated for both CPI ($n = 20$) and WPF ($n = 53$) watershed samples. Data was analyzed for normality using the Shapiro-Wilk test and for homogeneity of variance using Levene's test in R. Wilcoxon rank-sum tests were used to analyze differences in MAAT, peatland cover, and DOC between watershed types and to analyze the box plots in Figures 3–5. To explore the effect of interactions between watershed type and peatland cover, mixed-effect analysis of covariance (ANCOVA) analyses were conducted for each measured variable. Prior to ANCOVA analysis, non-normal data were transformed where possible to reduce violations of both normality and homoscedasticity where Levene's test showed heteroscedasticity (Olejnik & Algina, 1984). Specifically, average mass, NOSC, CHO (% RA), high O/C HUPs (% RA), Condensed aromatics (CA) (% RA), and polyphenolics (% RA) were square root transformed and CHOS (% RA), CHON (% RA), low O/C HUPs, aliphatic (% RA), and peptide-like (% RA) were log transformed. CHONS (% RA) was unable to be normalized using transformation. Results were considered statistically significant based on a $p$ value threshold of 0.05 and are presented both in the text and in Table S1 in Supporting Information S1.

## 3. Results

### 3.1. MAAT, Peatland Cover, and DOC Concentration

Mean annual air temperature (MAAT) ranged from $-7.22$ to $2.67°C$ across all sampled watersheds with an overall average of $-1.26$ °C for the entire region (Table 1). WPF watersheds were significantly warmer than CPI watersheds by an average of $5.68°C$ ($p < 0.005$, Table 1). Peatland cover ranged from 0 to $\sim76\%$ coverage overall (mean $= 38.8\% \pm 22.8\%$) and our sampling design captured approximately equal ranges of peatland cover across both WPF and CPI watersheds ($p = 0.77$, Table 1, Figure 2a). DOC ranged from 2.67 to 66.58 mg L$^{-1}$ across all samples (mean $= 25.70 \pm 18.89$ mg L$^{-1}$; Table 1) and appears to be highest where MAAT is near zero, with the maximum measured concentration occurring in a watershed with an average MAAT of 0.34 °C (Figure 2b). WPF watersheds had approximately five times more DOC on average than CPI watersheds ($32.81 \pm 17.39$ and $6.86 \pm 3.09$ mg L$^{-1}$, respectively, $p < 0.005$). DOC increased with peatland cover percentage in WPF watersheds only ($p < 0.005$, Figure 2b) and exhibited higher variance among WPF sites than in CPI sites ($p < 0.005$, Table 2).

### 3.2. DOM Composition

Negative-ion ESI FT-ICR MS at 21 T detected between 9,752 and 15,486 molecular formulae (mean $= 13,346 \pm 1,137$) across all samples, with no significant differences between WPF (mean $= 13,311 \pm 1,059$) and CPI ($13,439 \pm 1,348$) watersheds ($p = 0.145$, Table 1). There was no significant effect of peatland cover on number of molecular assignments ($p = 0.145$) or of watershed type alone ($p = 0.056$); however, there was a significant interaction between watershed type and peatland cover ($p = 0.016$), where a greater number of molecular formulae were identified from CPI watersheds and a lower number of molecular formulae from WPF watersheds as peatland cover increased. The average molecular weight of all singly charged $m/z$ ratios was $558.13 \pm 26.29$ Da and tended to be highest around $0°C$, with the maximum mass observed in a watershed with an average MAAT of $-0.22°C$ (Figure 3a), similar to the maximum DOC concentration. WPF watersheds and CPI watersheds exhibited DOM with statistically similar average mass ($565.93 \pm 22.89$ and $537.46 \pm 23.78$ Da, respectively, $p = 0.472$, Table 1, Figure 3b), and peatland cover did not appear to impact average mass in CPI

**Table 1**
*Mean Annual Air Temperature, Peatland Cover, DOC Concentration, and Dissolved Organic Matter Composition Data for West Siberia*

| Variable | Total ($n = 73$) Mean ± SD | WPF ($n = 53$) Mean ± SD | CPI ($n = 20$) Mean ± SD |
|---|---|---|---|
| MAAT (°C) | −1.26 ± 2.75 | 0.29 ± 0.99 | −5.39 ± 1.13 |
| Peatland Cover (%) | 38.8 ± 22.8 | 38.1 ± 23.3 | 40.6 ± 21.8 |
| DOC (mg L$^{-1}$) | 25.70 ± 18.89 | 32.81 ± 17.39 | 6.86 ± 3.09 |
| Number of molecular formulae | 13,346 ± 1,137 | 13,311 ± 1,059 | 13,439 ± 1,348 |
| Average Mass (Da) | 558.13 ± 26.29 | 565.93 ± 22.89 | 537.46 ± 23.78 |
| AI$_{mod}$ | 0.31 ± 0.03 | 0.31 ± 0.03 | 0.31 ± 0.02 |
| NOSC | −0.02 ± 0.08 | 0.00 ± 0.08 | −0.08 ± 0.05 |
| CHO (% RA) | 79.79 ± 7.60 | 80.60 ± 7.85 | 77.66 ± 6.59 |
| CHOS (% RA) | 6.70 ± 5.77 | 5.36 ± 3.99 | 10.27 ± 8.01 |
| CHON (% RA) | 13.30 ± 4.08 | 13.78 ± 4.51 | 12.02 ± 2.23 |
| CHONS (% RA) | 0.21 ± 0.53 | 0.27 ± 0.61 | 0.06 ± 0.09 |
| HUPs, High O/C (% RA) | 50.12 ± 6.15 | 52.62 ± 4.89 | 43.50 ± 3.82 |
| HUPs, Low O/C (% RA) | 32.03 ± 5.74 | 31.13 ± 5.78 | 34.42 ± 5.02 |
| Condensed Aromatics (% RA) | 1.77 ± 0.52 | 1.70 ± 0.51 | 1.96 ± 0.49 |
| Polyphenolics (% RA) | 10.78 ± 2.38 | 10.58 ± 2.66 | 11.33 ± 1.27 |
| CA + PP (% RA) | 12.55 ± 2.90 | 12.28 ± 3.17 | 13.29 ± 1.76 |
| Aliphatics (% RA) | 5.12 ± 4.78 | 3.79 ± 2.78 | 8.63 ± 6.90 |
| Peptide-like (% RA) | 0.14 ± 0.18 | 0.15 ± 0.21 | 0.12 ± 0.08 |
| Aliphatics + PL (% RA) | 5.26 ± 4.96 | 3.94 ± 2.99 | 8.75 ± 6.98 |

*Note.* Condensed aromatics and polyphenolics are combined and abbreviated as CA + PP, and Peptide-like is abbreviated as PL. MAAT, Peatland cover, and DOC are presented from Frey and Smith (2005).

watersheds (Figure 3a, Figure S1a in Supporting Information S1). However, average mass increased with higher peatland cover in WPF regions, with significant ANCOVA results from both peatland cover ($p < 0.005$) and interaction between peatland cover and permafrost ($p = 0.036$, Figure S1a in Supporting Information S1). The average AI$_{mod}$, an indicator of the presence of aromatic structures (Kellerman et al., 2018; Koch & Dittmar, 2006, 2015), was 0.31 ± 0.03 and was similar between watershed types ($p = 0.409$, Table 1; Figures 3c and 3d), but generally decreased with decreasing peatland coverage ($p < 0.005$, Figure 3c). There was no significant interaction between watershed type and peatland coverage with respect to AI$_{mod}$ ($p = 0.134$, Figure S1b in Supporting Information S1). NOSC, a qualitative indicator of the oxidation state of organic matter where higher values have been correlated with lower bioavailability in aerobic environments (Drake et al., 2018; Zhou et al., 2019), averaged −0.02 ± 0.08 (Figure 3e) and was slightly higher in WPF watersheds than in CPI watersheds, although this difference was not significant (mean = 0.0 ± 0.08 and −0.08 ± 0.05, respectively, $p = 0.538$, Table 1; Figure 3f). There was no significant effect of either peatland cover ($p = 0.413$), or peatland cover and watershed type ($p = 0.627$, Figure S1c in Supporting Information S1) with respect to NOSC.

The RA of molecular formulae classified as CHO ranged from 56.50 to 90.0 %RA overall (mean = 79.79 ± 7.60 %RA, Table 1; Figure 4a). CHO %RA was similar between watershed types ($p = 0.628$, Table 1; Figure 4b). CHO %RA increased with peatland cover ($p < 0.005$, Figure 4a), but there was no significant interaction between peatland cover and watershed type ($p = 0.093$, Figure S2a in Supporting Information S1). CHOS %RA ranged from 2.30 to 33.47 %RA (mean = 6.70 ± 5.77 %RA, Table 1; Figure 4c). CHOS %RA was similar between watershed types (mean = 10.28 ± 8.01 %RA, $p = 0.360$, Table 1; Figure 4d) but exhibited marginally higher variance in CPI watersheds ($p = 0.05$, Table 2). CHOS %RA decreased as peatland cover increased ($p < 0.005$) but there was no significant interaction between peatland cover and watershed type ($p = 0.14$, Figure S2b in Supporting Information S1). Across all samples, the %RA of CHON compounds ranged from 6.53 to 23.93 %RA
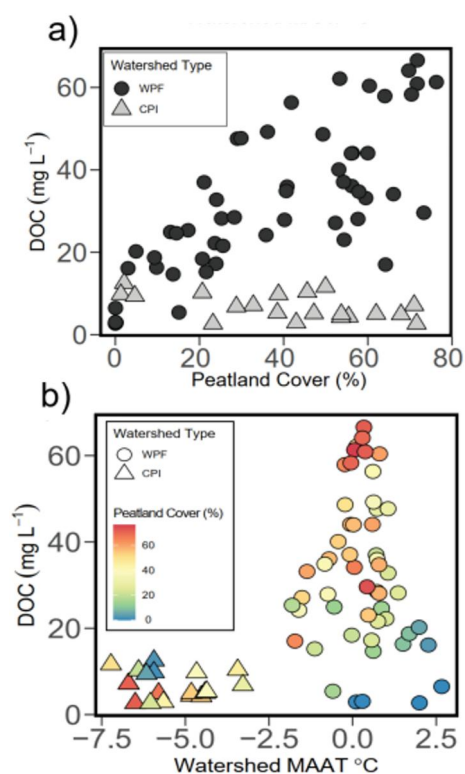
## Journal of Geophysical Research: Biogeosciences

**Figure 2.** Variation in DOC concentration across landscape-level drivers in rivers in West Siberia. Panel (a) depicts DOC (mg L$^{-1}$) versus peatland cover (%), and (b) depicts DOC (mg L$^{-1}$) versus watershed mean annual air temperature (°C) with peatland cover (%) overlaid as a colored scale, with cooler colors (blue) indicating less peatland cover and warmer colors (red) indicating greater peatland cover. Warm permafrost-free watersheds are depicted as circles and cold permafrost-influenced (CPI) CPI watersheds are depicted as triangles. Data replotted from Frey and Smith (2005).

(mean = 13.30 ± 4.08, Table 1; Figure 4e). CHON %RA was significantly higher in WPF watersheds (mean = 13.78 ± 4.51) compared to CPI watersheds (mean = 12.02 ± 2.23, $p < 0.005$, Table 1; Figure 4f). CHON %RA decreased as peatland cover increased in WPF watersheds only (Figure 4e), with significant effects of both peatland cover ($p < 0.005$) and peatland cover and watershed type together ($p = 0.009$, Figure S2c in Supporting Information S1). The variance in CHON %RA between watershed types was also higher in WPF watersheds ($p < 0.005$, Table 2). The least abundant compound class, CHONS, ranged from 0.00 to 3.13 %RA (mean = 0.21 ± 0.53) across all samples (Table 1; Figure 4g). The %RA of CHONS was higher in WPF watersheds (mean 0.27 ± 0.61 %RA), than in CPI watersheds (mean 0.06 ± 0.09 %RA), but due to the high variability in WPF watersheds, this relationship was not statistically significant ($p = 0.06$, Table 1; Figure 4h; Figure S2d in Supporting Information S1). The %RA of CHONS decreased as peatland area increased ($p = 0.008$), but there was no significant interaction between watershed type and peatland cover ($p = 0.186$).

Across all samples, high O/C HUPs ranged from 30.33 to 58.92 %RA (mean = 50.12 ± 6.15 %RA, Table 1; Figure 5a). High O/C HUPs were significantly more abundant in WPF watersheds (mean = 52.62 ± 4.89 %RA) than in CPI watersheds (mean = 43.50 ± 3.82 %RA, $p = 0.038$, Table 1; Figure 5b). The %RA of high O/C HUPs increased with increasing peatland cover ($p = 0.009$), but this appeared to be limited to WPF watersheds (Figure 5a). However, the effect of permafrost and peatland cover interactions on high O/C HUPs was not statistically significant ($p = 0.073$, Figure S3a in Supporting Information S1). Low O/C HUPs ranged from 22.50 to 55.38 %RA for the entire dataset (mean = 32.03 ± 5.74 %RA, Table 1; Figure 5c). The %RA of low O/C HUPs was similar between watershed types (Table 1; $p = 0.157$, Figure 5d). Peatland cover had a negative relationship with low O/C HUPs ($p = 0.009$), and this appeared to be limited to WPF watersheds only (Figure 5c) with a significant interaction between peatland cover and watershed type ($p = 0.003$, Figure S3b in Supporting Information S1). Condensed aromatics (CA) and polyphenolics (PP) are both markers of terrestrially-sourced DOM (Kurek et al., 2022; Wagner et al., 2015) and therefore are presented here grouped together as CA + PP, ranged from 4.15 to 17.75 %RA (mean = 12.55 ± 2.84 %RA, Table 1; Figure 5e). Peatland cover appeared to increase the %RA of these formulae ($p < 0.005$), specifically in WPF samples (Figure 5e) with a significant interaction between peatland cover and watershed type ($p = 0.029$, Figure S3c in Supporting Information S1). Conversely to CA + PP, peptide-like (PL) and aliphatic formulae represent markers of in situ or microbial DOM and have been shown to be linked to biolabile DOM (Drake et al., 2018; Kellerman et al., 2018; Spencer et al., 2015; Textor et al., 2019) and are presented here combined as PL + Aliphatics. The %RA of these typically autochthonous and microbial markers ranged from 2.02 to 28.98 %RA (mean = 5.26 ± 4.96 %RA) overall (Figure 5g). CPI watersheds had a significantly higher %RA of PL + Aliphatics than WPF watersheds ($p = 0.03$, Table 1; Figure 5h). The %RA of PL + Aliphatics decreased with increasing peatland cover ($p < 0.005$, Figure 5g). There was no significant effect of the interaction between peatland cover and watershed type on PL + Aliphatic %RA ($p = 0.396$, Figure S3d in Supporting Information S1).

To further examine relationships between landscape variables and DOM composition within the dataset, a PCA encompassing DOC concentration and FT-ICR MS parameters was performed (Figure 6). PC1, driven by AI$_{mod}$, average mass, CHO %RA, NOSC, and PL + Aliphatics %RA explained 51.7% of the variance (Figure 6a, Table S2 in Supporting Information S1) and appears to correlate with increasing peatland cover from left to right along PC1 (Figure 6b). PC2 explained 19.7% of the variance and was driven by high O/C HUPs, CHON, CHONS, and PL + Aliphatics %RA (Figure 6a, Table S2 in Supporting Information S1). PC2 appears to correlate with permafrost influence, with CPI watersheds separating along the axis of PC2, regardless of peatland cover (Figure 6b).

**Table 2**
*Variance Analysis for All Measured Parameters*

| | WPF variance ($s^2$) | CPI variance ($s^2$) | Levene's test $p$ value |
|---|---|---|---|
| MAAT (°C) | 0.98 | 1.27 | 0.241 |
| Peatland Cover (%) | 542.4 | 475.7 | 0.288 |
| DOC (mg L$^{-1}$) | 302.37 | 9.57 | **<0.005** |
| Number of molecular formulae | 1,120,520 | 1,817,080 | 0.657 |
| Average Mass (Da) | 524.07 | 565.68 | 0.367 |
| AI$_{mod}$ | 0 | 0 | 0.547 |
| NOSC | 0.01 | 0 | 0.417 |
| CHO (% RA) | 61.58 | 43.49 | 0.382 |
| CHOS (% RA) | 15.9 | 64.2 | **0.050** |
| CHON (% RA) | 20.33 | 4.96 | **<0.005** |
| CHONS (% RA) | 0.37 | 0.01 | 0.128 |
| HUPs, High O/C (% RA) | 23.87 | 14.6 | 0.742 |
| HUPs, Low O/C (% RA) | 33.38 | 25.18 | 0.891 |
| Condensed Aromatics (% RA) | 0.27 | 0.24 | 0.843 |
| Polyphenolics (% RA) | 7.1 | 1.6 | **0.040** |
| CA + PP (% RA) | 9.84 | 2.84 | 0.063 |
| Aliphatics (% RA) | 7.74 | 47.62 | **0.012** |
| Peptide-like (% RA) | 0.04 | 0.01 | 0.264 |
| Aliphatics + PL (% RA) | 8.16 | 47.19 | **0.016** |

*Note.* Statistically significant $p$ values (< 0.05) are represented with bold type face. MAAT, Peatland cover, and DOC are presented from Frey and Smith (2005).

## 4. Discussion

### 4.1. Characterizing Riverine DOM in West Siberian Watersheds

We found marked differences in DOM composition varying with both permafrost influence and peatland cover, with peatland cover driving high variance in permafrost-free watersheds but not permafrost-influenced watersheds, which displayed relatively low, stable variance. This signifies that warming-induced changes to Arctic land cover and soil characteristics are likely to increase not only the amount of DOC transported by West Siberian rivers as reported previously (Frey & Smith, 2005), but also the overall heterogeneity of DOM composition. CPI watershed DOM was generally characterized by lower DOC concentration, a lower %RA of CHON classified molecular formulae and high O/C HUPs, and a greater %RA of PL + Aliphatic classed compounds (Table 1; Figures 2b, 4f, 5f, and 5h). The relative increase in the %RA of high H/C and PL + Aliphatics is typical of the molecular signature for permafrost soil-derived DOM (Spencer et al., 2015; Stubbins et al., 2017; Textor et al., 2019), and therefore may be indicative of potential inputs from permafrost thaw and subsequent transport of permafrost-derived DOM into CPI watersheds. The higher %RA of aliphatics also suggests that CPI watershed DOM may have greater biolability than that of WPF watersheds, as previous research suggests that aliphatic DOM inputs from permafrost thaw are often rapidly biodegraded (D'Andrilli et al., 2015; Spencer et al., 2015; Textor et al., 2019).

WPF watershed DOM exhibited greater variability in DOC concentration, %RA CHOS, CHON, and polyphenolics (Table 2). This variability in molecular signature highlights the heterogeneity of DOM sources across permafrost-free West Siberian ecosystems. These results suggest a greater diversity of soil layer and groundwater inputs in rivers that drain permafrost-free watersheds versus those with permafrost influence, as well as the potential for more microbial degradation in the longer residence time flow paths of WPF watersheds (Behnke et al., 2021). Human impacts have the potential to further increase the diversity of these inputs; warming temperatures, forest fires, and shifting precipitation regimes are implicated in vegetation changes like forest and shrub expansion, or Arctic greening (Kirpotin et al., 2021; Myers-Smith et al., 2020). It can be
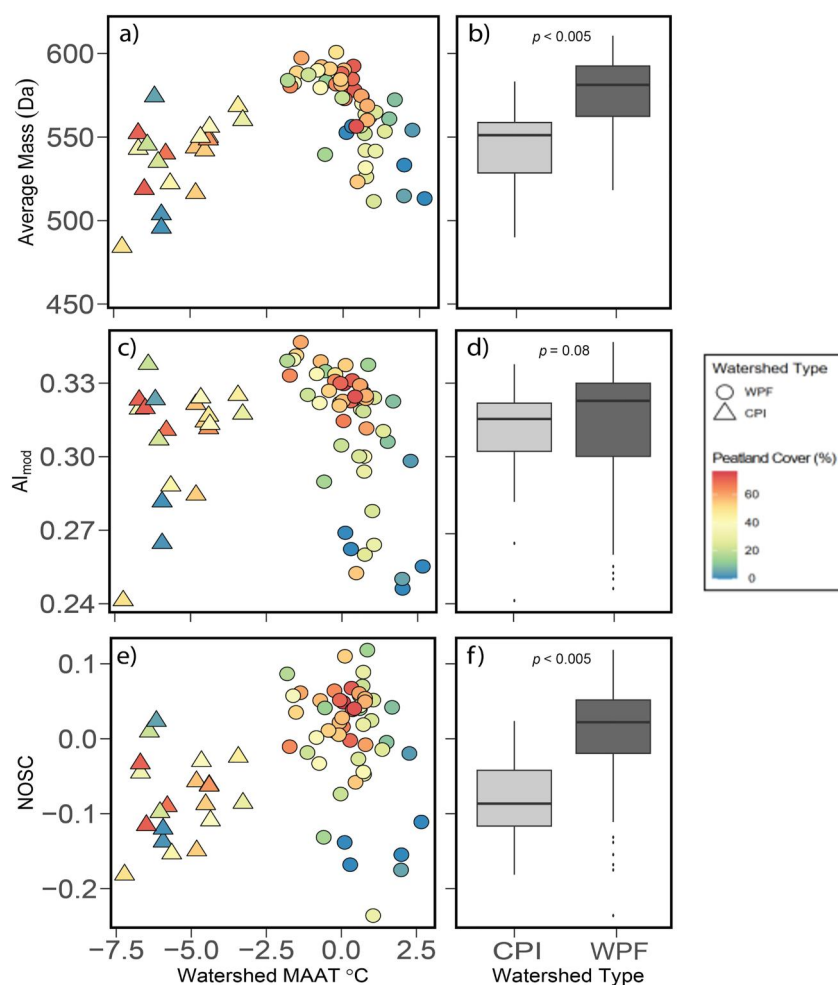
**Figure 3.** Average Mass (Da), AI$_{mod}$, and nominal oxidation state of carbon (NOSC). In the left column, variables are presented against watershed mean annual air temperature (°C). Triangles indicate cold permafrost-influenced (CPI) watersheds and circles indicate warm permafrost-free (WPF) watersheds. Color represents peatland cover (%), with cooler colors (blue) indicating lower coverage and warmer colors (red) indicating greater coverage. In the right column, box plots for each variable are presented for each watershed type (CPI vs. WPF), where the lower and upper box hinges correspond to the 25th and 75th percentiles, and the horizontal line within the box represents the median. Wilcoxon rank sum test results are presented on the box plot panels.

expected that Arctic DOM will become increasingly heterogeneous as permafrost thaw and vegetation changes continue into the future, providing a greater variety of DOM sources and longer watershed residence times enabling greater microbial degradation of DOM (Behnke et al., 2021). This heterogeneity represents a greater variety of both available metabolic substrate and stable compounds and has implications for greenhouse gas production and storage as DOM is exported from the landscape toward the Arctic Ocean.

### 4.2. Peatland or Permafrost: Identifying Controls on Riverine DOM

As peatland cover increases across both permafrost-free and permafrost-influenced watersheds, average mass, AI$_{mod}$ and the %RA of CHO, CHOS, high O/C HUPs, and CA + PP increased concurrently, while the %RA of CHON and PL + Aliphatics decreased (Figures S1a, S1b, S2a, S2b, S3a, S3c, and S3d in Supporting Information S1). This indicates that peatland cover acts as a control not only on DOC concentration in surface waters (Xenopoulos et al., 2003) but also with respect to DOM composition, specifically through contributions of more terrestrial DOM with higher average mass. This agrees with other observations from both peat porewater, which has been shown to have high aromaticity and molecular weight (Prijac et al., 2022; Tfaily et al., 2013), and from data collected from the largest Arctic rivers, where the Ob' River, which contains the greatest peatland area of all
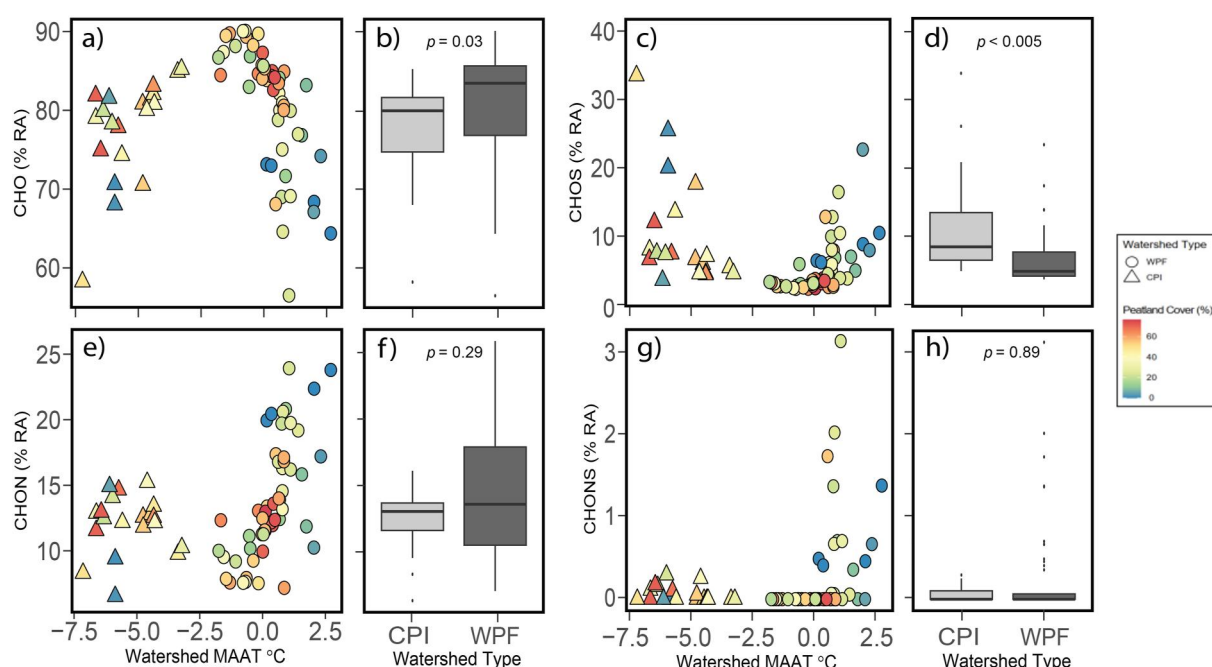
**Figure 4.** Relative abundance (%) of heteroatom classes against watershed mean annual air temperature (°C) and box plots for watershed type (cold permafrost-influenced (CPI) vs. warm permafrost-free (WPF)): (a) CHO, (b) CHO box plot, (c) CHOS, (d) CHOS box plot, (e) CHON, (f) CHON box plot, (g) CHONS, (h) CHONS box plot. Triangles indicate CPI watersheds and circles indicate WPF watersheds. Color represents peatland cover (%), with cooler colors (blue) indicating lower coverage and warmer colors (red) indicating greater coverage. Box plots for each variable are presented for each watershed type (CPI vs. WPF), where the lower and upper box hinges correspond to the 25th and 75th percentiles, and the horizontal line within the box represents the median. Wilcoxon rank sum test results are presented on the box plot panels.

six major Arctic watersheds, is observed to export the most aromatic DOM (Amon et al., 2012; Behnke et al., 2021). Furthermore, Arctic watersheds such as the Severnaya Dvina and Onega that have extensive peatland coverage have been shown to export DOM that is even more aromatic in nature and exhibit higher average mass DOM than that found in the major Arctic rivers with comparatively less peatland cover in their watersheds (Johnston et al., 2018; Starr et al., 2023). Despite being an important control on riverine DOM, difficulties in delineating Arctic wetland area, predicting changes to total peatland area, and limited data from northern high-latitude peatlands constrain attempts to scale these impacts to DOM export from the Pan-Arctic watershed. While the impacts of permafrost thaw on riverine DOM composition have been the focus of many research efforts, the data presented here clearly highlights the need to improve estimates of peatland cover change in order to better predict Arctic carbon dynamics.

Across these watersheds, past research highlighted that permafrost effectively shuts down the influence of peatland cover on DOC concentration (Frey & Smith, 2005). Our results find a similar control with respect to permafrost on DOM composition. Peatland cover and permafrost influence showed significant interactions on several of our measured variables, including average mass and the %RA of CHON, low O/C HUPs, and CA + PP. These variables are controlled by peatland cover only in WPF watersheds, with average mass and CA + PP %RA increasing with peatland cover, and CHON and low O/C HUPs decreasing as peatland cover increases (Figures 4e, 5c, and 5e, respectively). However, the absence of effects from peatland cover on these variables in CPI watersheds suggests that the presence of permafrost is a paramount control on the impact of peatland cover on some aspects of DOM composition. Put simply, in the CPI watersheds the presence of permafrost does not allow the variability of peatland cover to manifest an influence over DOM composition as is apparent in the WPF watersheds.

Furthermore, given the clustering of high peatland cover sites at the positive end of PC1 (Figure 6), peatland cover appeared to explain more than half of the variance in DOM. This alone might suggest that peatland cover is a more important driver of DOM characteristics than permafrost influence in West Siberia. However, despite the apparent stronger control of peatlands on riverine DOM that emerged in the PCA, permafrost appears to act as a switch controlling the influence of peatlands. Thus, it stands to reason that as the Arctic continues to warm, peatland cover
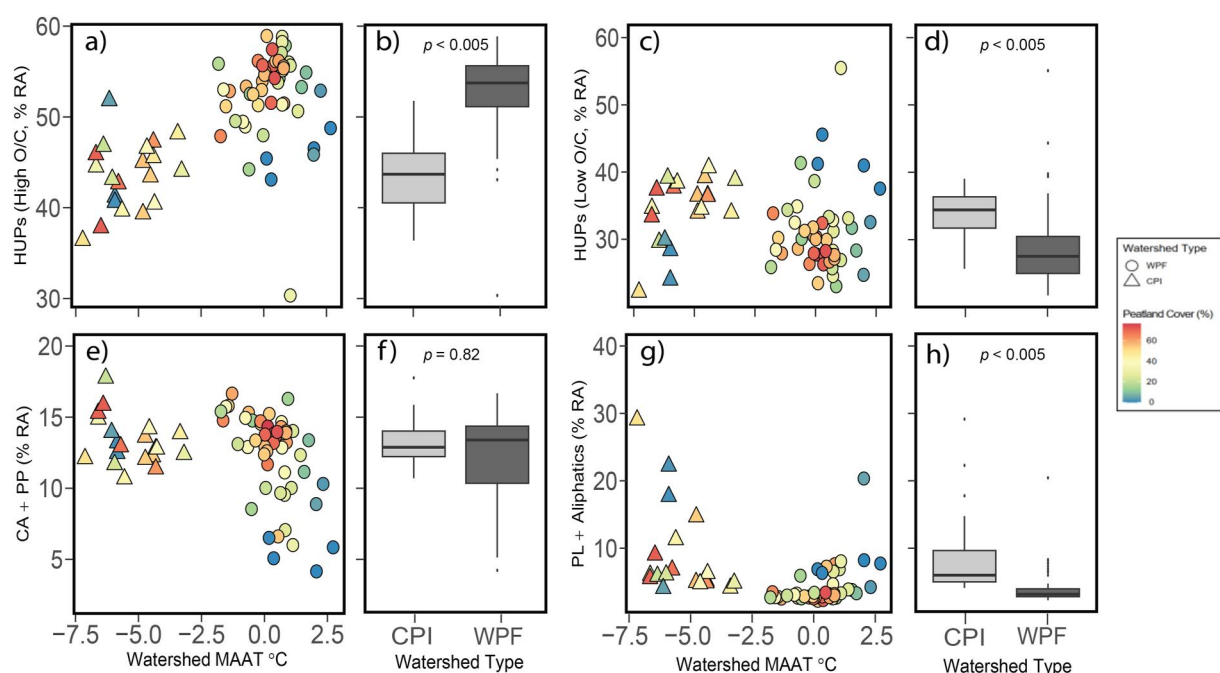
**Figure 5.** Relative abundance (%) of compound classes against watershed mean annual air temperature (°C) and box plots for watershed type (cold permafrost-influenced (CPI) vs. warm permafrost-free (WPF)): (a) HUPs (High O/C), (b) HUPs (High O/C) box plot, (c) HUPs (Low O/C), (d) HUPs (Low O/C) box plot, (e) Condensed aromatics (CA) and polyphenolics (CA + PP), (f) CA + PP box plot, (g) peptide-like (PL) and aliphatics, (h) PL + Aliphatics box plot. Triangles indicate CPI watersheds and circles indicate WPF watersheds. Color represents peatland cover (%), with cooler colors (blue) indicating lower coverage and warmer colors (red) indicating greater coverage. Box plots for each variable are presented for each watershed type (CPI vs. WPF), where the lower and upper box hinges correspond to the 25th and 75th percentiles, and the horizontal line within the box represents the median. Wilcoxon rank sum test results are presented on the box plot panels.

will become a more important control on DOM composition in watersheds previously influenced by permafrost, as rising temperatures and permafrost thaw unlock the influence of peat cover on riverine DOM composition.

### 4.3. Predicting the Fate of West Siberian DOM Under Future Warming

Using a space-for-time approach to analyze DOM compositional changes under continued warming, we suggest that DOM in systems currently underlain by permafrost may start to resemble the DOM signature of WPF sites. Greater DOC concentrations in WPF watersheds compared to CPI watersheds suggest that West Siberia may follow the observed trend of increasing surface water DOC concentrations with continued warming in both West Siberia (Frey & Smith, 2005; Krickov et al., 2018) and across other Arctic regions (Shogren et al., 2019; Tank et al., 2016; Toohey et al., 2016). Importantly, our data suggest that warming may increase not only the amount of DOC but also the heterogeneity of DOM exported by West Siberian rivers. However, some of our measured variables appear to reach maximum or minimum values around 0°C MAAT, such as DOC concentration, average mass, NOSC, and the %RA of CHO and high O/C HUPs (Figures 3a, 3c, 4a, and 5a). This apparent pattern may represent production or export limitation as observed by Laudon et al. (2012), or a balance between production and respiration in West Siberian rivers. Thus, potential shifts in DOM composition in Siberian watersheds may be limited to a certain range of warming, and may potentially reverse as temperatures continue to warm. Despite this, we posit that under continued warming and permafrost thaw, West Siberian DOM will likely undergo the following changes:

1. Peatland influence will become a more important control on DOM composition as permafrost thaws. As surface hydrology increasingly interacts with subsurface and groundwater systems (e.g., Frey, McClelland, et al., 2007; Smith et al., 2007) under continued permafrost degradation, OC rich peatland soils will become available for leaching and export in watersheds previously influenced by permafrost.
2. DOM composition in rivers will have greater heterogeneity as the influence of peatland cover is amplified across the landscape. Some parameters that will become more variable include average mass, heteroatom content (e.g., CHON, CHONS), and aromaticity.
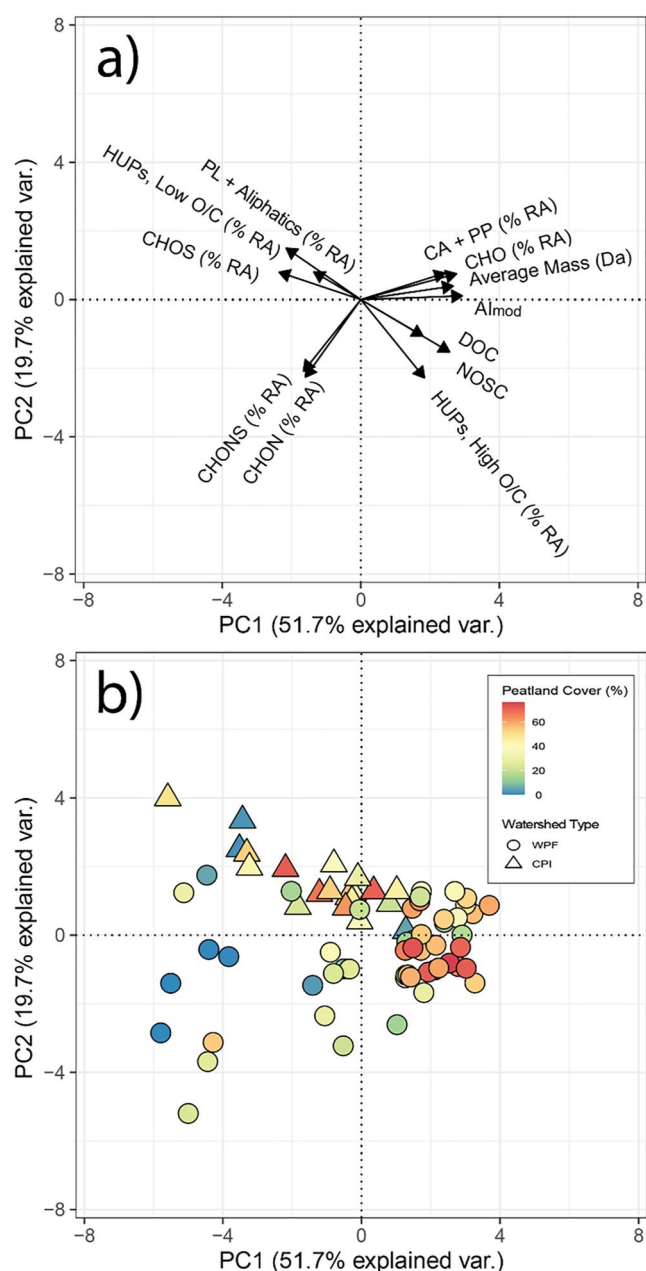
**Figure 6.** Principal component analysis (PCA) of compositional parameters in West Siberian watershed samples showing (a) the loadings for each variable and (b) the individual samples plotted on the PCA. Triangles indicate cold permafrost-influenced watersheds and circles indicate warm permafrost-free watersheds. Color represents peatland cover (%), with cooler colors (blue) indicating lower coverage and warmer colors (red) indicating greater coverage.

3. West Siberian DOM compositions will likely shift toward higher average mass, an increasing %RA of high O/C HUPs, and a decreasing %RA of aliphatic and peptide-like compounds in warming Arctic watersheds. These shifts in DOM composition may have ramifications for the fate of exported material (D'Andrilli et al., 2015; Kaiser et al., 2017; Spencer et al., 2015; Textor et al., 2019), including potentially a greater role for photochemical degradation (Bowen et al., 2020; Grunert et al., 2021; Ward & Cory, 2016). Thus, we suggest that the Arctic Ocean may receive relatively more high molecular weight DOM from freshwater inputs as warming continues and that exported DOM may be more susceptible with respect to photochemical degradation processes.

Ultimately, these shifts in DOM composition depend on the balance of changing sources from permafrost inputs to peatland dominance and so, in the short-term, an increase in relatively biolabile DOM export may be observed concurrent with increasing permafrost thaw until permafrost stores are depleted in the watersheds and peatland stable DOM export becomes the dominant process. As higher molecular weight, more aromatic peatland DOM may also be more susceptible to photochemical degradation, these exports may be tempered by photochemical degradation in transit as aromatic moieties have been observed to be susceptible to UV irradiation (Bowen et al., 2020; Wagner et al., 2018; Ward & Cory, 2016). Changes in pH, temperature, nutrient availability, and other abiotic factors, as well as changes in microbial activity and community composition, can also alter the chemical transformation of exported DOM (O'Donnell et al., 2016b; Timko et al., 2015; Young et al., 2005); thus, our predictions based solely on changes in DOM composition represent just one part of a complex and rapidly changing question. It is readily apparent that future research efforts are required that couple DOM composition analysis with microbial and hydrochemical analyses to better delineate future controls on DOM processing and fate.

These observed shifts in DOM composition are an important component of a changing Arctic carbon cycle, as DOM is an important substrate for biogeochemical transformation and a potential source of greenhouse gas emissions. Permafrost thaw is predicted to also impact soil characteristics, OC storage, and greenhouse gas emissions in Arctic and boreal peatlands (Bruhwiler et al., 2021; Kåresdotter et al., 2021; Kreplin et al., 2021). For example, in permafrost-influenced peatlands in Canada, thaw is predicted to increase OC accumulation and net carbon storage rates while also increasing net radiative forcing through increased methane emissions (Turetsky et al., 2007). Furthermore, there is a large amount of uncertainty in predicting how peatland cover will change under continuing permafrost thaw. Arctic wetland areas have been projected to both shrink and expand with permafrost thaw (Bruhwiler et al., 2021; Kreplin et al., 2021) and predicting which will occur is hindered by high landscape heterogeneity across the Pan-Arctic watershed and limitations in delineating wetlands. Establishing a consensus on the changing export and fate of DOM in the Arctic is as also limited by sparse long-term monitoring efforts, especially in smaller catchments and outside of usual field seasons (Shogren et al., 2020; Starr et al., 2023). Efforts to scale predicted OC storage and emissions from warming peatlands to the entire Pan-Arctic region are constrained by this uncertainty. Understanding the interactions between permafrost and peatlands and their combined effects on DOM composition, and thus its role in the environment, is necessary for understanding carbon cycling in the Arctic as warming continues. This study illustrates the entwined nature of the control peatlands and permafrost may have on Arctic carbon cycles, and how thawing permafrost and warming peatlands may impact the composition of DOM exported to downstream fluvial, lacustrine, and marine ecosystems.

## Conflict of Interest

The authors declare no conflicts of interest relevant to this study.

## Data Availability Statement

All 21 T FT-ICR MS mass spectra files and elemental compositions are publicly available via the Open Science Framework (https://osf.io/ka5d7/) at https://doi.org/10.17605/OSF.IO/Q46TS.

## References

Aitkenhead, J. A., & McDowell, W. H. (2000). Soil C:N ratio as a predictor of annual riverine DOC flux at local and global scales. *Global Biogeochemical Cycles*, *14*(1), 127–138. https://doi.org/10.1029/1999GB900083

Amon, R. M. W., Rinehart, A. J., Duan, S., Louchouarn, P., Prokushkin, A., Guggenberger, G., et al. (2012). Dissolved organic matter sources in large Arctic rivers. *Geochimica et Cosmochimica Acta*, *94*, 217–237. https://doi.org/10.1016/J.GCA.2012.07.015

Barnes, R. T., Smith, R. L., & Aiken, G. R. (2012). Linkages between denitrification and dissolved organic matter quality, Boulder Creek watershed, Colorado. *Journal of Geophysical Research*, *117*(G1), 1014. https://doi.org/10.1029/2011JG001749

Behnke, M. I., McClelland, J. W., Tank, S. E., Kellerman, A. M., Holmes, R. M., Haghipour, N., et al. (2021). Pan-Arctic riverine dissolved organic matter: Synchronous molecular stability, shifting sources and subsidies. *Global Biogeochemical Cycles*, *35*(4), e2020GB006871. https://doi.org/10.1029/2020GB006871

Benner, R., Louchouarn, P., & Amon, R. M. W. (2005). Terrigenous dissolved organic matter in the Arctic Ocean and its transport to surface and deep waters of the North Atlantic. https://doi.org/10.1029/2004GB002398

Blakney, G. T., Hendrickson, C. L., & Marshall, A. G. (2011). Predator data station: A fast data acquisition system for advanced FT-ICR MS experiments. *International Journal of Mass Spectrometry*, *306*(2–3), 246–252. https://doi.org/10.1016/J.IJMS.2011.03.009

Bowen, J. C., Kaplan, L. A., & Cory, R. M. (2020). Photodegradation disproportionately impacts biodegradation of semi-labile DOM in streams. *Limnology & Oceanography*, *65*(1), 13–26. https://doi.org/10.1002/lno.11244

Brown, J. (1998). *National Snow and Ice Data Center*. World Data Center for Glaciology.

Bruhwiler, L., Parmentier, F.-J. W., Crill, P., Leonard, M., & Palmer, P. I. (2021). The Arctic carbon cycle and its response to changing climate. https://doi.org/10.1007/s40641-020-00169-5/Published

Chanton, J. P., Glaser, P. H., Chasar, L. S., Burdige, D. J., Hines, M. E., Siegel, D. I., et al. (2008). Radiocarbon evidence for the importance of surface vegetation on fermentation and methanogenesis in contrasting types of boreal peatlands. *Global Biogeochemical Cycles*, *22*(4). https://doi.org/10.1029/2008GB003274

Chaudhary, N., Westermann, S., Lamba, S., Shurpali, N., Sannel, A. B. K., Schurgers, G., et al. (2020). Modelling past and future peatland carbon dynamics across the pan-Arctic. *Global Change Biology*, *26*(7), 4119–4133. https://doi.org/10.1111/GCB.15099

Clark, J. B., Mannino, A., Tzortziou, M., Spencer, R. G. M., & Hernes, P. (2022). The transformation and export of organic carbon across an arctic river-delta-ocean continuum. *Journal of Geophysical Research: Biogeosciences*, *127*(12). https://doi.org/10.1029/2022JG007139

Corilo, Y. (2015). EnviroOrg [Software]. *Florida State University*.

D'Andrilli, J., Cooper, W. T., Foreman, C. M., & Marshall, A. G. (2015). An ultrahigh-resolution mass spectrometry index to estimate natural organic matter lability. *Rapid Communications in Mass Spectrometry*, *29*(24), 2385–2401. https://doi.org/10.1002/RCM.7400

Dittmar, T., Koch, B., Hertkorn, N., & Kattner, G. (2008). A simple and efficient method for the solid-phase extraction of dissolved organic matter (SPE-DOM) from seawater. *Limnology and Oceanography: Methods*, *6*, 230–235. https://doi.org/10.4319/LOM.2008.6.230

Drake, T. W., Guillemette, F., Hemingway, J. D., Chanton, J. P., Podgorski, D. C., Zimov, N. S., & Spencer, R. G. M. (2018). The ephemeral signature of permafrost carbon in an Arctic fluvial network. *Journal of Geophysical Research: Biogeosciences*, *123*(5), 1475–1485. https://doi.org/10.1029/2017JG004311

Drake, T. W., Wickland, K. P., Spencer, R. G. M., McKnight, D. M., & Striegl, R. G. (2015). Ancient low-molecular-weight organic acids in permafrost fuel rapid carbon dioxide production upon thaw. *Proceedings of the National Academy of Sciences of the U S A*, *112*(45), 13946–13951. https://doi.org/10.1073/pnas.1511705112

Fabre, C., Sauvage, S., Tananaev, N., Noël, G. E., Teisserenc, R., Probst, J., & Pérez, J. S. (2019). Assessment of sediment and organic carbon exports into the Arctic Ocean: The case of the Yenisei River basin. *Water Research*, *158*, 118–135. https://doi.org/10.1016/J.WATRES.2019.04.018

Fenner, N., Freeman, C., & Worrall, F. (2009). Hydrological controls on dissolved organic carbon production and release from UK peatlands. In *Carbon cycling in northern peatlands* (Vol. 184, pp. 237–249).

Fewster, R. E., Morris, P. J., Ivanovic, R. F., Swindles, G. T., Peregon, A. M., & Smith, C. J. (2022). Imminent loss of climate space for permafrost peatlands in Europe and Western Siberia. *Nature Climate Change*, *12*(4 12), 373–379. https://doi.org/10.1038/s41558-022-01296-7

Frey, K. E., & McClelland, J. W. (2009). Impacts of permafrost degradation on arctic river biogeochemistry. *Hydrological Processes*, *23*(1), 169–182. https://doi.org/10.1002/hyp.7196

Frey, K. E., McClelland, J. W., Holmes, R. M., & Smith, L. G. (2007). Impacts of climate warming and permafrost thaw on the riverine transport of nitrogen and phosphorus to the Kara Sea. *Journal of Geophysical Research*, *112*(G4), 4–58. https://doi.org/10.1029/2006JG000369

Frey, K. E., Siegel, D. I., & Smith, L. C. (2007). Geochemistry of west Siberian streams and their potential response to permafrost degradation. *Water Resources Research*, *43*(3). https://doi.org/10.1029/2006WR004902

Frey, K. E., & Smith, L. C. (2005). Amplified carbon release from vast West Siberian peatlands by 2100. *Geophysical Research Letters*, *32*(9), 1–4. https://doi.org/10.1029/2004GL022025

Friborg, T., Soegaard, H., Christensen, T. R., Lloyd, C. R., & Panikov, N. S. (2003). Siberian wetlands: Where a sink is a source. *Geophysical Research Letters*, *30*(21), 2129. https://doi.org/10.1029/2003GL017997

Frolking, S., Talbot, J., Jones, M. C., Treat, C. C., Kauffman, J. B., Tuittila, E. S., & Roulet, N. (2011). Peatlands in the Earth's 21st century climate system. *Environmental Reviews*, *19*(NA), 371–396. https://doi.org/10.1139/a11-014

Gallego-Sala, A. V., Charman, D. J., Brewer, S., Page, S. E., Prentice, I. C., Friedlingstein, P., et al. (2018). Latitudinal limits to the predicted increase of the peatland carbon sink with warming. *Nature Climate Change*, *8*(10 8), 907–913. https://doi.org/10.1038/s41558-018-0271-1

Gandois, L., May Hoyt, A., Hatté, C., Jeanneau, L., Teisserenc, R., Liotaud, M., & Tananaev, N. (2019). Contribution of peatland permafrost to dissolved organic matter along a thaw gradient in North Siberia. *Technology*, *53*(24), 14165–14174. https://doi.org/10.1021/acs.est.9b03735i

Grunert, B. K., Tzortziou, M., Neale, P., Menendez, A., & Hernes, P. (2021). DOM degradation by light and microbes along the Yukon River-coastal ocean continuum. *Scientific Reports*, *11*(1), 10236. https://doi.org/10.1038/s41598-021-89327-9

Hall, L. J., Emilson, E. J. S., Edwards, B., & Watmough, S. A. (2021). Patterns and trends in lake concentrations of dissolved organic carbon in a landscape recovering from environmental degradation and widespread acidification. *Science of the Total Environment*, *765*, 142679. https://doi.org/10.1016/J.SCITOTENV.2020.142679

Hendrickson, C. L., Quinn, J. P., Kaiser, N. K., Smith, D. F., Blakney, G. T., Chen, T., et al. (2015). 21 Tesla Fourier transform ion cyclotron resonance mass spectrometer: A national resource for ultrahigh resolution mass analysis. *Journal of the American Society for Mass Spectrometry*, *26*(9), 1626–1632. https://doi.org/10.1007/s13361-015-1182-2

Hugelius, G., Loisel, J., Chadburn, S., Jackson, R. B., Jones, M., MacDonald, G., et al. (2020). Large stocks of peatland carbon and nitrogen are vulnerable to permafrost thaw. *Proceedings of the National Academy of Sciences of the United States of America*, *117*(34), 20438–20446. https://doi.org/10.1073/PNAS.1916387117

IPCC. (2023). Climate change 2023: Synthesis report.

Jiao, N., Herndl, G. J., Hansell, D. A., Benner, R., Kattner, G., Wilhelm, S. W., et al. (2010). Microbial production of recalcitrant dissolved organic matter: Long-term carbon storage in the global ocean. *Nature Reviews Microbiology*, *8*(8 8), 593–599. https://doi.org/10.1038/nrmicro2386

Johnston, S. E., Shorina, N., Bulygina, E., Vorobjeva, T., Chupakova, A., Klimov, S. I., et al. (2018). Flux and seasonality of dissolved organic matter from the Northern Dvina (Severnaya Dvina) River, Russia. *Journal of Geophysical Research: Biogeosciences*, *123*(3), 1041–1056. https://doi.org/10.1002/2017JG004337

Juhls, B., Stedmon, C. A., Morgenstern, A., Meyer, H., Hölemann, J., Heim, B., et al. (2020). Identifying drivers of seasonality in Lena River biogeochemistry and dissolved organic matter fluxes. *Frontiers in Environmental Science*, *8*, 53. https://doi.org/10.3389/FENVS.2020.00053/BIBTEX

Kaiser, K., Benner, R., & Amon, R. M. W. (2017). The fate of terrigenous dissolved organic carbon on the Eurasian shelves and export to the North Atlantic. *Journal of Geophysical Research: Oceans*, *122*(1), 4–22. https://doi.org/10.1002/2016JC012380

Kåresdotter, E., Destouni, G., Ghajarnia, N., Hugelius, G., & Kalantari, Z. (2021). Mapping the vulnerability of arctic wetlands to global warming. *Earth's Future*, *9*(5), e2020EF001858. https://doi.org/10.1029/2020EF001858

Kellerman, A. M., Kothawala, D. N., Dittmar, T., & Tranvik, L. J. (2015). Persistence of dissolved organic matter in lakes related to its molecular characteristics. *Nature Geoscience*, *8*(6), 454–457. https://doi.org/10.1038/NGEO2440

Kellerman, A. M., Guillemette, F., Podgorski, D. C., Aiken, G. R., Butler, K. D., & Spencer, R. G. M. (2018). Unifying concepts linking dissolved organic matter composition to persistence in aquatic ecosystems. https://doi.org/10.1021/acs.est.7b05513

Kirpotin, S. N., Callaghan, T. V., Peregon, A. M., Babenko, A. S., Berman, D. I., Bulakhova, N. A., et al. (2021). Impacts of environmental change on biodiversity and vegetation dynamics in Siberia. *Ambio*, *50*(11), 1926–1952. https://doi.org/10.1007/S13280-021-01570-6/FIGURES/9

Koch, B. P., & Dittmar, T. (2006). From mass to structure: An aromaticity index for high-resolution mass data of natural organic matter. *Rapid Communications in Mass Spectrometry*, *20*(5), 926–932. https://doi.org/10.1002/RCM.2386

Koch, B. P., & Dittmar, T. (2015). From mass to structure: An aromaticity index for high-resolution mass data of natural organic matter. https://doi.org/10.1002/rcm.2386

Kortelainen, P., Mattsson, T., Finér, L., Ahtiainen, M., Saukkonen, S., & Sallantaus, T. (2006). Controls on the export of C, N, P and Fe from undisturbed boreal catchments, Finland. *Aquatic Sciences*, *68*(4), 453–468. https://doi.org/10.1007/S00027-006-0833-6

Kreplin, H. N., Santos Ferreira, C. S., Destouni, G., Keesstra, S. D., Salvati, L., & Kalantari, Z. (2021). Arctic wetland system dynamics under climate warming. *Wiley Interdisciplinary Reviews: Water*, *8*(4), e1526. https://doi.org/10.1002/WAT2.1526

Krickov, I. V., Lim, A. G., Manasypov, R. M., Loiko, S. V., Shirokova, L. S., Kirpotin, S. N., et al. (2018). Riverine particulate C and N generated at the permafrost thaw front: Case study of western Siberian rivers across a 1700 km latitudinal transect. *Biogeosciences*, *15*(22), 6867–6884. https://doi.org/10.5194/BG-15-6867-2018

Kurek, M. R., Stubbins, A., Drake, T. W., Dittmar, T., M. S. Moura, J., Holmes, R. M., et al. (2022). Organic molecular signatures of the Congo River and comparison to the Amazon. *Global Biogeochemical Cycles*, *36*(6), e2022GB007301. https://doi.org/10.1029/2022GB007301

Laudon, H., Buttle, J., Carey, S. K., McDonnell, J., McGuire, K., Seibert, J., et al. (2012). Cross-regional prediction of long-term trajectory of stream water DOC response to climate change. *Geophysical Research Letters*, *39*(18). https://doi.org/10.1029/2012GL053033

Lim, A. G., Loiko, S. V., & Pokrovsky, O. S. (2022). Sizable pool of labile organic carbon in peat and mineral soils of permafrost peatlands, western Siberia. *Geoderma*, *409*, 115601. https://doi.org/10.1016/J.GEODERMA.2021.115601

Lin, H., Xu, H., Cai, Y., Belzile, C., Macdonald, R. W., & Guo, L. (2021). Dynamic changes in size-fractionated dissolved organic matter composition in a seasonally ice-covered Arctic River. *Limnology & Oceanography*, *66*(8), 3085–3099. https://doi.org/10.1002/LNO.11862

Loisel, J., Gallego-Sala, A. V., Amesbury, M. J., Magnan, G., Anshari, G., Beilman, D. W., et al. (2020). Expert assessment of future vulnerability of the global peatland carbon sink. *Nature Climate Change*, *11*(1), 70–77. https://doi.org/10.1038/s41558-020-00944-0

Mann, P. J., Spencer, R. G. M., Dinga, B. J., Poulsen, J. R., Hernes, P. J., Fiske, G., et al. (2014). The biogeochemistry of carbon across a gradient of streams and rivers within the Congo Basin. *Journal of Geophysical Research: Biogeosciences*, *119*(4), 687–702. https://doi.org/10.1002/2013JG002442

Moore, T. R. (2009). Dissolved organic carbon production and transport in Canadian peatlands. In *Carbon cycling in northern peatlands* (Vol. 184, pp. 229–236).

Morris, P. J., Swindles, G. T., Valdes, P. J., Ivanovic, R. F., Gregoire, L. J., Smith, M. W., et al. (2018). Global peatland initiation driven by regionally asynchronous warming. *Proceedings of the National Academy of Sciences of the United States of America*, *115*(19), 4851–4856. https://doi.org/10.1073/PNAS.1717838115/SUPPL_FILE/PNAS.1717838115.SD02.CSV

Myers-Smith, I. H., Kerby, J. T., Phoenix, G. K., Bjerke, J. W., Epstein, H. E., Assmann, J. J., et al. (2020). Complexity revealed in the greening of the Arctic. *Nature Climate Change*, *10*(2 10), 106–117. https://doi.org/10.1038/s41558-019-0688-1

Natali, S. M., Holdren, J. P., Rogers, B. M., Treharne, R., Duffy, P. B., Pomerance, R., & MacDonald, E. (2021). Permafrost carbon feedbacks threaten global climate goals. *Proceedings of the National Academy of Sciences*, *118*(21), e2100163118. https://doi.org/10.1073/pnas.171783811

New, M., Hulme, M., & Jones, P. (1999). Representing twentieth-century space–time climate variability. Part I: Development of a 1961–90 mean monthly terrestrial climatology. *Journal of Climate*, *12*(3), 829–856. https://doi.org/10.1175/1520-0442(1999)012

O'Donnell, J. A., Aiken, G. R., Butler, K. D., Guillemette, F., Podgorski, D. C., & Spencer, R. G. M. (2016). DOM composition and transformation in boreal forest soils: The effects of temperature and organic-horizon decomposition state. *Journal of Geophysical Research: Biogeosciences*, *121*(10), 2727–2744. https://doi.org/10.1002/2016jg003431

O'Donnell, J. A., Aiken, G. R., Swanson, D. K., Panda, S., Butler, K. D., & Baltensperger, A. P. (2016). Dissolved organic matter composition of Arctic rivers: Linking permafrost and parent material to riverine carbon. *Global Biogeochemical Cycles*, *30*(12), 1811–1826. https://doi.org/10.1002/2016GB005482

Oksanen, J., Blanchet, F. G., Friendly, M., Kidnt, R., Legendre, P., McGlinn, D., et al. (2020). Package "vegan" title community ecology package. Version 2.5-7.

Olejnik, S. F., & Algina, J. (1984). Parametric ANCOVA and the rank transform ANCOVA when the data are conditionally non-normal and heteroscedastic. *Journal of Educational Statistics*, *9*(2), 129–149. https://doi.org/10.2307/1164717

Pokrovsky, O. S., Manasypov, R. M., Kopysov, S. G., Krickov, I. V., Shirokova, L. S., Loiko, S. V., et al. (2020). Impact of permafrost thaw and climate warming on riverine export fluxes of carbon, nutrients and metals in Western Siberia. *Water*, *12*(6), 1817. https://doi.org/10.3390/W12061817

Pokrovsky, O. S., Manasypov, R. M., Loiko, S., Shirokova, L. S., Krickov, I. A., Pokrovsky, B. G., et al. (2015). Permafrost coverage, watershed area and season control of dissolved carbon and major elements in western Siberian rivers. *Biogeosciences*, *12*(21), 6301–6320. https://doi.org/10.5194/bg-12-6301-2015

Prijac, A., Gandois, L., Jeanneau, L., Taillardat, P., & Garneau, M. (2022). Dissolved organic matter concentration and composition discontinuity at the peat-pool interface in a boreal peatland. *Biogeosciences*, *19*(18), 4571–4588. https://doi.org/10.5194/BG-19-4571-2022

Qiu, C., Ciais, P., Zhu, D., Guenet, B., Chang, J., Chaudhary, N., et al. (2022). A strong mitigation scenario maintains climate neutrality of northern peatlands. *One Earth*, *5*(1), 86–97. https://doi.org/10.1016/j.oneear.2021.12.008

Raudina, T. V., Loiko, S. V., Lim, A. G., Krickov, I. V., Shirokova, L. S., Istigechev, G. I., et al. (2017). Dissolved organic carbon and major and trace elements in peat porewater of sporadic, discontinuous, and continuous permafrost zones of western Siberia. *Biogeosciences*, *14*, 3561–3584. https://doi.org/10.5194/BG-14-3561-2017

Riedel, T., Biester, H., & Dittmar, T. (2012). Molecular fractionation of dissolved organic matter with metal salts. *Environmental Science & Technology*, *46*(8), 50–4426. https://doi.org/10.1021/es203901u

Roth, H. K., Borch, T., Young, R. B., Bahureksa, W., Blakney, G. T., Nelson, A. R., et al. (2022). Enhanced speciation of pyrogenic organic matter from wildfires enabled by 21 T FT-ICR mass spectrometry. *Analytical Chemistry*, *94*(6), 2973–2980. https://doi.org/10.1021/ACS.ANALCHEM.1C05018/SUPPL_FILE/AC1C05018_SI_002.PDF

Savory, J. J., Kaiser, N. K., Mckenna, A. M., Xian, F., Blakney, G. T., Rodgers, R. P., et al. (2011). Parts-per-billion Fourier transform ion cyclotron resonance mass measurement accuracy with a "walking" calibration equation. *Analytical Chemistry*, *83*(5), 59–1736. https://doi.org/10.1021/ac102943z

Schuur, E. A. G., Abbott, B. W., Bowden, W. B., Brovkin, V., Camill, P., Canadell, J. G., et al. (2013). Expert assessment of vulnerability of permafrost carbon to climate change. *Climate Change*, *119*(2), 359–374. https://doi.org/10.1007/S10584-013-0730-7/FIGURES/2

Schuur, E. A. G., Abbott, B. W., Commane, R., Ernakovich, J., Euskirchen, E., Hugelius, G., et al. (2022). Permafrost and climate change: Carbon cycle feedbacks from the warming Arctic. *Annual Review of Environment and Resources*, *47*(1), 343–371. https://doi.org/10.1146/ANNUREV-ENVIRON-012220-011847

Schuur, E. A. G., Bockheim, J., Canadell, J. G., Euskirchen, E., Field, C. B., Goryachkin, S. V., et al. (2008). Vulnerability of permafrost carbon to climate change: Implications for the global carbon cycle. *BioScience*, *58*(8), 701–714. https://doi.org/10.1641/b580807

Schuur, E. A. G., McGuire, A. D., Schädel, C., Grosse, G., Harden, J. W., Hayes, D. J., et al. (2015). Climate change and the permafrost carbon feedback. *Nature*, *520*(7546), 171–179. https://doi.org/10.1038/nature14338

Sepp, M., Kõiv, T., Nõges, P., & Nõges, T. (2019). The role of catchment soils and land cover on dissolved organic matter (DOM) properties in temperate lakes. https://doi.org/10.1016/j.jhydrol.2019.01.012

Sheng, Y., Smith, L. C., MacDonald, G. M., Kremenetski, K. V., Frey, K. E., Velichko, A. A., et al. (2004). A high-resolution GIS-based inventory of the west Siberian peat carbon pool. *Global Biogeochemical Cycles*, *18*(3). https://doi.org/10.1029/2003GB002190

Shogren, A. J., Zarnetske, J. P., Abbott, B. W., Iannuci, F., Frei, R. J., Griffin, N. A., & Bowden, W. B. (2019). Revealing biogeochemical signatures of Arctic landscapes with river chemistry. https://doi.org/10.1038/s41598-019-49296-6

Shogren, A. J., Zarnetske, J. P., Abbott, B. W., Iannucci, F., & Bowden, W. B. (2020). We cannot shrug off the shoulder seasons: Addressing knowledge and data gaps in an Arctic headwater. *Environmental Research Letters*, *15*(10), 104027. https://doi.org/10.1088/1748-9326/AB9D3C

Smith, D. F., Podgorski, D. C., Rodgers, R. P., Blakney, G. T., & Hendrickson, C. L. (2018). 21 Tesla FT-ICR mass spectrometer for ultrahigh-resolution analysis of complex organic mixtures. *Analytical Chemistry*, *90*(3), 2041–2047. https://doi.org/10.1021/ACS.ANALCHEM.7B04159/ASSET/IMAGES/ACS.ANALCHEM.7B04159.SOCIAL.JPEG_V03

Smith, L. C., MacDonald, G. M., Velichko, A. A., Beilman, D. W., Borisova, O. K., Frey, K. E., et al. (2004). Siberian peatlands a net carbon sink and global methane source since the Early Holocene. *Science*, *303*(5656), 353–356. https://doi.org/10.1126/SCIENCE.1090553/SUPPL_FILE/SMITH.SOM.PDF

Smith, L. C., Pavelsky, T. M., MacDonald, G. M., Shiklomanov, A. I., & Lammers, R. B. (2007). Rising minimum daily flows in northern Eurasian rivers: A growing influence of groundwater in the high-latitude hydrologic cycle. *Journal of Geophysical Research*, *112*(G4). https://doi.org/10.1029/2006JG000327

Smith, L. C., Sheng, Y., MacDonald, G. M., & Hinzman, L. D. (2005). Atmospheric science: Disappearing Arctic lakes. *Science*, *308*(5727), 1429. https://doi.org/10.1126/SCIENCE.1108142/SUPPL_FILE/SMITH-SOM.PDF

Spencer, R. G. M., Ahad, J. M. E., Baker, A., Cowie, G. L., Ganeshram, R., Upstill-Goddard, R. C., & Uher, G. (2007). The estuarine mixing behaviour of peatland derived dissolved organic carbon and its relationship to chromophoric dissolved organic matter in two North Sea estuaries (U.K.). https://doi.org/10.1016/j.ecss.2007.03.032

Spencer, R. G. M., Mann, P. J., Dittmar, T., Eglinton, T. I., McIntyre, C., Holmes, R. M., et al. (2015). Detecting the signature of permafrost thaw in Arctic rivers. *Geophysical Research Letters*, *42*(8), 2830–2835. https://doi.org/10.1002/2015GL063498.Received

Starr, S., Johnston, S. E., Sobolev, N., Perminova, I., Kellerman, A., Fiske, G., et al. (2023). Characterizing uncertainty in Pan-Arctic land-ocean dissolved organic carbon flux: Insights from the Onega River, Russia. *Journal of Geophysical Research: Biogeosciences*, *128*(5), e2022JG007073. https://doi.org/10.1029/2022JG007073

Striegl, R. G., Aiken, G. R., Dornblaser, M. M., Raymond, P. A., & Wickland, K. P. (2005). A decrease in discharge-normalized DOC export by the Yukon River during summer through autumn. *Geophysical Research Letters*, *32*(21), 1–4. https://doi.org/10.1029/2005GL024413

Stubbins, A., Mann, P. J., Powers, L., Bittar, T. B., Dittmar, T., McIntyre, C. P., et al. (2017). Low photolability of yedoma permafrost dissolved organic carbon. *Journal of Geophysical Research: Biogeosciences*, *122*(1), 200–211. https://doi.org/10.1002/2016JG003688

Tank, S. E., Striegl, R. G., McClelland, J. W., & Kokelj, S. V. (2016). Multi-decadal increases in dissolved organic carbon and alkalinity flux from the Mackenzie drainage basin to the Arctic Ocean. *Environmental Research Letters*, *11*(5), 054015. https://doi.org/10.1088/1748-9326/11/5/054015

Terhaar, J., Lauerwald, R., Regnier, P., Gruber, N., & Bopp, L. (2021). Around one third of current Arctic Ocean primary production sustained by rivers and coastal erosion. *Nature Communications*, *12*, 1–10. https://doi.org/10.1038/s41467-020-20470-z

Textor, S. R., Wickland, K. P., Podgorski, D. C., Johnston, S. E., & Spencer, R. G. M. (2019). Dissolved organic carbon turnover in permafrost-influenced watersheds of Interior Alaska: Molecular Insights and the priming effect. *Frontiers in Earth Science*, *7*, 275. https://doi.org/10.3389/FEART.2019.00275/BIBTEX

Tfaily, M. M., Hamdan, R., Corbett, J. E., Chanton, J. P., Glaser, P. H., & Cooper, W. T. (2013). Investigating dissolved organic matter decomposition in northern peatlands using complimentary analytical techniques. *Geochimica et Cosmochimica Acta*, *112*. https://doi.org/10.1016/j.gca.2013.03.002

Timko, S. A., Gonsior, M., & Cooper, W. J. (2015). Influence of pH on fluorescent dissolved organic matter photo-degradation. *Water Research*, *85*, 266–274. https://doi.org/10.1016/j.watres.2015.08.047

Toohey, R. C., Herman-Mercer, N. M., Schuster, P. F., Mutter, E. A., & Koch, J. C. (2016). Multidecadal increases in the Yukon River Basin of chemical fluxes as indicators of changing flowpaths, groundwater, and permafrost. *Geophysical Research Letters*, *43*(23), 12120–12130. https://doi.org/10.1002/2016GL070817

Turetsky, M. R., Wieder, R. K., Vitt, D. H., Evans, R. J., & Scott, K. D. (2007). The disappearance of relict permafrost in boreal north America: Effects on peatland carbon storage and fluxes. *Global Change Biology*, *13*(9), 1922–1934. https://doi.org/10.1111/J.1365-2486.2007.01381.X

Wagner, S., Jaffé, R., Cawley, K., Dittmar, T., & Stubbins, A. (2015). Associations between the molecular and optical properties of dissolved organic matter in the Florida Everglades, a model coastal wetland system. *Frontiers in Chemistry*, *3*, 66. https://doi.org/10.3389/FCHEM.2015.00066/BIBTEX

Wagner, S., Jaffé, R., & Stubbins, A. (2018). Dissolved black carbon in aquatic ecosystems. *Limnology and Oceanography Letters*, *3*(3), 168–185. https://doi.org/10.1002/lol2.10076

Walker, S. A., Amon, R. M. W., & Stedmon, C. A. (2013). Variations in high-latitude riverine fluorescent dissolved organic matter: A comparison of large Arctic rivers. *Journal of Geophysical Research: Biogeosciences*, *118*(4), 1689–1702. https://doi.org/10.1002/2013JG002320

Ward, C. P., & Cory, R. M. (2016). Complete and partial photo-oxidation of dissolved organic matter draining permafrost soils. *Environmental Science & Technology*, *50*(7), 3545–3553. https://doi.org/10.1021/acs.est.5b05354

Wild, B., Andersson, A., Bröder, L., Vonk, J., Hugelius, G., McClelland, J. W., et al. (2019). Rivers across the Siberian Arctic unearth the patterns of carbon release from thawing permafrost. *Proceedings of the National Academy of Sciences of the United States of America*, *116*(21), 10280–10285. https://doi.org/10.1073/pnas.1811797116

Xenopoulos, M. A., Lodge, D. M., Frentress, J., Kreps, T. A., Bridgham, S. D., Grossman, E., & Jackson, C. J. (2003). Regional comparisons of watershed determinants of dissolved organic carbon in temperate lakes from the Upper Great Lakes region and selected regions globally. *Limnology & Oceanography*, *48*(6), 2321–2334. https://doi.org/10.4319/LO.2003.48.6.2321

Xian, F., Hendrickson, C. L., Blakney, G. T., Beu, S. C., & Marshall, A. G. (2010). Automated broadband phase correction of Fourier transform ion cyclotron resonance mass spectra. *Analytical Chemistry*, *82*(21), 8807–8812. https://doi.org/10.1021/AC101091W

Young, K. C., Docherty, K. M., Maurice, P. A., & Bridgham, S. D. (2005). Degradation of surface-water dissolved organic matter: Influences of DOM chemical characteristics and microbial populations. *Hydrobiologia*, *539*, 1–11. https://doi.org/10.1007/s10750-004-3079-0

Zhou, C., Liu, Y., Liu, C., & Tfaily, M. M. (2019). Compositional changes of dissolved organic carbon during its dynamic desorption from hyporheic zone sediments. *Science of the Total Environment*, *658*, 16–23. https://doi.org/10.1016/J.SCITOTENV.2018.12.189